ON GENERATING SPECIAL QUASIRANDOM STRUCTURES: OPTIMIZATION FOR THE DFT COMPUTATIONAL EFFICIENCY*

Andrzej P. Kądzielawa

AGH University of Krakow, Faculty of Physics and Applied Computer Science
al. A. Mickiewicza 30, 30-059 Kraków, Poland
andrzej.kadzielawa@agh.edu.pl

Received 11 February 2026, accepted 16 March 2026, published online 15 May 2026

We present our novel evolutionary algorithm for generating Special Quasirandom Structures (SQS) designed to optimize the computational efficiency of Density Functional Theory (DFT) computations. Operating on the premise that symmetry proxies non-randomness, we rigorously filter out 1.P1 candidate structures prior to evaluating correlation functions. Our extinction-based workflow includes the seeding, filtration, evaluation, extinction, and repopulation phases to produce efficient supercells with maximal local environmental distinctness. We compare our results against those generated by established software packages, on the example of the $W_{70}Cr_{30}$ alloy. Although standard tools achieve (marginally) lower correlation errors, our best-performing structures require approximately five times fewer unique displacements for phonon calculations. This approach sacrifices negligible quantitative disorder accuracy to significantly reduce the computational cost of modeling thermal properties.

DOI:10.5506/APhysPolB.57.5-A15

1. Introduction

In recent years, there has been a growing incentive for the exploration of compositionally complex and disordered systems. This transition is driven by the urgent demand for materials capable of withstanding extreme environments (*e.g.*, the so-called Lost-of-coolant accident — LOCA), particularly in applications of fusion energy [1, 2] and nuclear shielding [3–7]. It made the stochastic arrangement of atoms a primary design variable, which is exemplified by the rise of High-Entropy Alloys (HEAs) [8–15] and refractory-metal alloys [16–26], where stabilization of the entropy and local chemical tuning are critical. However, the theoretical treatment of such systems

* Presented at the Concepts in Strongly Correlated Quantum Matter Conference (CSCQM), Kraków, Poland, 20–22 November, 2025.

presents a major obstacle: a computational complexity overtaking the existent HPC resources, *i.e.*, the modeling of thermal properties (necessary for alloys) and their stability, requires more resources than those available. The current state-of-the-art *ab-initio* tools are based on Density Functional Theory (DFT) [27–33], which provides a robust quantum mechanical framework. The reliance on translational symmetry contradicts the intrinsic nature of disordered alloys. The Special Quasirandom Structure (SQS) method [34–36] resolves this issue by constructing finite periodic supercells that mimic the disorder of an infinite random alloy. Given that the computational cost of DFT scales cubically with the size of the system ($O(N^3)$), the central optimization problem is not only minimizing the correlation error in the infinite limit, but identifying the set of most computationally efficient optimized supercells that capture the essential physics.

In the latest developments, new SQS algorithms have been made available, together with their implementations, *e.g.*, SimplySQS by Lebeda *et al.* [37] or PyHEA by Niu and Liu [38]. Nevertheless, these approaches focus more on optimization of the workflow (via massive parallelization using GPU [38] with the impressive 250,000-atom supercells) or user experience (through a web-based framework [37]). Although their efficiency overshadows the state-of-the-art ATAT [39] and sqsgenerator [40], they do not change the underlying algorithm. In addition, frameworks such as AlloyGAN [41] and material network representations [42] employ deep learning to instantaneously construct valid alloy architectures, shifting the bottleneck entirely to the physical solver.

Previously, we showed that the focus on computational complexity when generating SQSs allows for incorporation of thermal effects that reproduce both miscibility gaps in the W–Cr–Mo binary systems [43] and predict the stability and elastic properties of the tungsten-based refractory-metal alloys (W–Cr–Ta/Hf) [44].

In this paper, we present our evolutionary approach that operates on the premise that symmetry is a proxy for non-randomness. By rigorously filtering out high-symmetry and redundant candidates before the computationally expensive evaluation of correlation functions, the algorithm accelerates the discovery of optimal structures. Crucially for DFT efficiency, this method produces small supercells with maximal local environmental distinctness. This trade-off, even though reducing the randomness globally, does not impact the local disorder "as seen" from a random lattice node. Moreover, this algorithm allows for coarse-grained, massively-parallel, stochastic implementation.

In Section 2, we describe the theoretical foundations of our approach, as well as the underlying algorithm. Then, in Section 3, we compare our resultant structures with those obtained from established software [39, 40], using the alloy $W_{70}Cr_{30}$ as an example. Finally, in Section 4, we summarize the findings presented in this paper.

2. Theoretical foundations of configurational disorder

In this chapter, we introduce a population-based evolutionary approach driven by an *extinction* mechanism.

2.1. The Cluster Expansion formalism

The basis of the SQS method is the *Cluster Expansion (CE)* formalism [45]. For a binary alloy $A_{1-x}B_x$, we assign a variable σ_i to each site i (*e.g.*, 0 for the atom A, 1 for the atom B). Any physical property P of a configuration $\vec{\sigma}$ can be expanded

$$P(\vec{\sigma}) = P_0 + \sum_{\alpha} P_\alpha \mathfrak{C}_\alpha(\vec{\sigma})\,. \tag{1}$$

Here, $\mathfrak{C}_\alpha(\vec{\sigma})$ is the structure-dependent correlation function for a cluster α. SQS generation is an optimization problem: finding a configuration $\vec{\sigma}$ in a supercell S such that

$$\mathfrak{C}_\alpha(S) \approx \mathfrak{C}_\alpha^{\text{rand}} \tag{2}$$

for all physically relevant clusters α.

2.2. Extinction-based generation method (pseudocode)

Although standard tools (*e.g.*, ATAT) often (and for large supercells almost exclusively) produce structures with $P1$ (lowest) symmetry, we aim at filtering for residual symmetries (*e.g.*, $C2$, $Amm2$). This decreases the number of irreducible displacements required for phonon calculations without introducing qualitative errors in the disordered limit, which leads to the possibility to apply the so-called quasiharmonic approximation (QHA) [46, 47] to obtain the high-temperature properties of an alloy.

The following Algorithm 1 defines *a generic* workflow to generate a set of SQSs using the extinction-based approach. Note that for the algorithm to function, we need to define the lattice type, supercell size, tolerance, and population size. The approach consists of five phases: *(i)* seeding, where the initial cells are generated; *(ii)* filtration, where the low-symmetry cells are filtered out; *(iii)* evaluation, where correlation/error functions are

calculated; *(iv)* extinction, where the worst performing cells are rejected; and *(v)* repopulation, where a new set of offspring cells is generated from the survivors.

Algorithm 1 Extinction-Based SQS Generator. This is the simplest possible algorithm. In general, we allow for a small $\ll P$ number of the best $P1$ structures modifying line 4. We also include a standard Metropolis algorithm [48] (with the reciprocal *temperature* β), to allow for some locally *nonoptimal* states, modifying 15.

Require: Lattice type L, Supercell size N, Tolerance $\mathfrak{E}_{tol}$, Population size P
Input: Concentrations $\{x_i\}$, Output size M

1: $Population \leftarrow \emptyset$
2: **while** LENGTH($Population$) $< M$ **do** ▷ *Phase i: Seeding*
3: $C \leftarrow$ GENERATERANDOMSUPERCELL($L, N, \{x_i\}$)
4: **if** SYMMETRY(C) $\neq P1$ **and** C is unique **then** ▷ *Phase ii: Filtration*
5: POPULATION.APPEND(C)
6: $\mathfrak{E}_{min} \leftarrow \infty$
7: **while** $\mathfrak{E}_{min} > \mathfrak{E}_{tol}$ **do** ▷ *Phase iii-v: Evolution*
8: **for** S_i in $Population$ **do** ▷ *Phase iii: Evaluation*
9: $S_i.\mathfrak{E} \leftarrow$ CALCCORRELATIONMISMATCH(S_i) ▷ $\mathfrak{E}$ *includes displacements.*
10: $\mathfrak{E}_{min} \leftarrow$ MIN($\mathfrak{E}_{min}, S_i.\mathfrak{E}$)
11: $D_{min} \leftarrow$ NUM_OF_UNIQUE_DISPLACEMENTS(S_i)
12: **if** $\mathfrak{E}_{min}/D_{min} \leq \mathfrak{E}_{tol}$ **then return** $Population$
13: $Survivors \leftarrow \emptyset$
14: **for** S_i in $Population$ **do** ▷ *Phase iv: Extinction*
15: $P_{survival} \leftarrow \mathfrak{E}_{min}/S_i.\mathfrak{E}$ ▷ *Can be replaced with* $\exp(-\beta(S_i.\mathfrak{E} - \mathfrak{E}_{min})$
16: **if** RANDOM(0,1) $\leq P_{survival}$ **then**
17: SURVIVORS.APPEND(S_i)
18: $Population \leftarrow Survivors$
19: **while** Length($Population$) $< P$ **do** ▷ *Phase v: Repopulation*
20: Parent $\leftarrow$ SELECTRANDOM(Survivors)
21: Offspring $\leftarrow$ MUTATE(Parent)
22: **if** SYMMETRY(Offspring)$\neq P1$ **then**
23: POPULATION.APPEND(Offspring)

Output: M Optimal SQS Structures

The separate calculation in Algorithm 1:9 is described in more detail as Algorithm 2. Note that the required weights A_n are a series of (typically) decreasing monotonically with n values that prioritize correlations for the nearest-neighbors. As there is no *ab-initio* form of A_n, we choose the power

form of $A_n \equiv \frac{1}{n}$. Tests with $A_n \equiv n^{-p}$, with $p \in \{2, 4, 12\}$ and $A_n = R_n^{-1}$ (R_n being the distance to the coordination zone) produced similar results for the $P1$ structures, but performed worse for computationally efficient supercells (with a convergence of the algorithm being of an order of magnitude slower).

Note that in Algorithm 2:22, we modify the error function to penalize structures with the large number of unique displacements required for the phononic spectrum computations. This ensures that Algorithm 1 uses the (computationally) cheaper structures, *cf.* the success condition in Algorithm 1:12 does not take the number of displacements into account. In the next section, we compare our results with those obtained with state-of-the-art tools.

Algorithm 2 Calculating error: `CalcCorrelationMismatch`

Require: Weights A_n
Input: Supercell, Concentrations x,
1: $BackgroundSupercell \leftarrow \emptyset$
2: $a, b, c = Supercell.directions$
3: **for** i,j,k in CARTHESIAN_PRODUCT($\{-1, 0, 1\}$, 3) **do**
4: **for** atom in Supercell **do**
5: $mirrorAtom \leftarrow atom$
6: $mirrorAtom.position \leftarrow atom.position + i\,a + j\,b + k\,c$
7: $BackgroundSupercell.append(mirrorAtom)$
8: $CoordZones \leftarrow$ FIND_COORDINATION_ZONES(Supercell,BackgroundSupercell)
9: **for** Zone in CoordZones **do**
10: **for** atomType in Zone.atomTypes **do**
11: $Zone[atomType].correlation \leftarrow 0$
12: **for** atomS in Supercell **do**
13: **for** atomB in BackgroundSupercell **do**
14: **if** atomS.type == atomB.type **then**
15: CoordZones.from_atoms(atomS,atomB)[atomB.type].correlation +=1
16: $\mathfrak{E} \leftarrow 0$
17: **for** n,Zone in ENUMERATE(CoordZones) **do**
18: **for** atomType in Zone.atomTypes **do**
19: $Zone[atomType].correlation /= Zone[atomType].population$
20: $Zone[atomType].correlation -= x[atomType]$
21: $\mathfrak{E} += A_n \times |Zone[atomType].correlation|$ ▷ *No || ⇌ error cancellation included*
22: $\mathfrak{E} *=$ NUM_OF_UNIQUE_DISPLACEMENTS(Supercell) ▷ *Optimization; This favors computationally "cheaper" supercells.*
Output: Mismatch magnitude $\mathfrak{E}$

3. Comparative analysis

In this section, we analyze the error function of our resultant supercells compared to those generated using the established software.

The key feature of the approach above is to *(i)* get a set of computationally effective supercells that still *(ii)* model the local disorder of an alloy (still being SQSs). While *(i)* is satisfied directly, to substantiate *(ii)*, we verify the "properness" of our SQSs by comparing them to those generated by established codes (here sqsgenerator [40] and ATAT [39]) in terms of the pure error function (without the inclusion of the number of displacements).

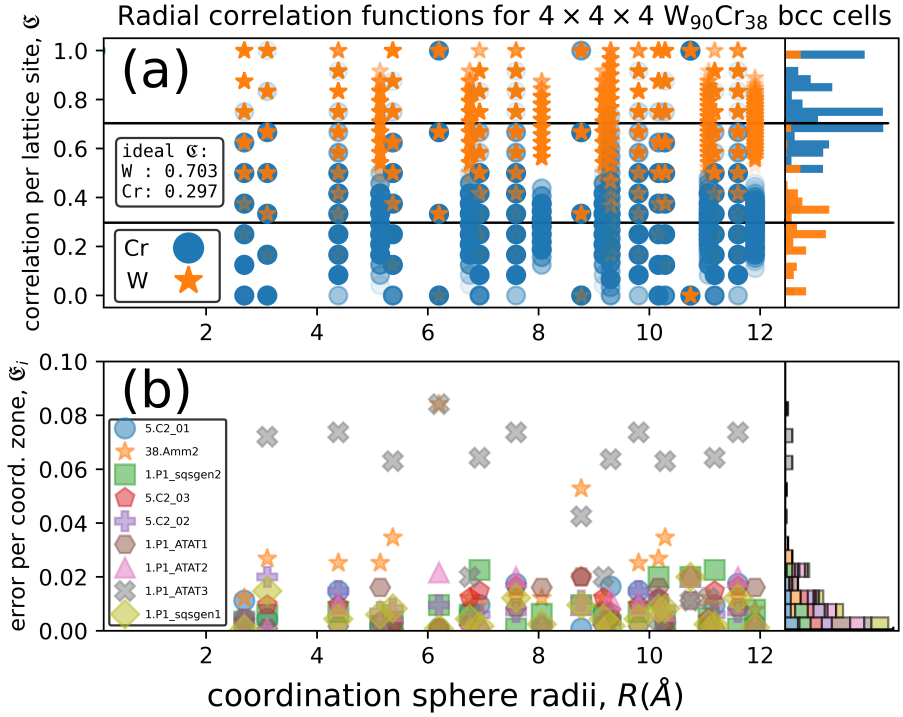

Fig. 1. Correlation (a) and error (b) functions for different $4 \times 4 \times 4$ bcc Special Quasirandom $W_{70}Cr_{30}$ Structures (exactly $W_{90}Cr_{38}$ supercell). Histograms on the right sum up the corresponding populations. We used two sqsgenerator [40] generated 1.P1-symmetry cells with 10^9 (1.P1_sqsgen1) and 10^9 (1.P1_sqsgen2) iterations, and three ATAT [39] 10^9 (1.P1_ATAT1 and 1.P1_ATAT2), and 10^2 (1.P1_ATAT3) iterations. We included our own cells from 5.C2 and 38.Amm2 symmetry groups, while the result for a purely random 1.P1 cell is given as a reference point. Note that, while 1.P1_ATAT1 (brown hexagons) is the best (error-wise with $\mathfrak{E} = 2.01 \times 10^{-4}$), our 5.C3_03 ($\mathfrak{E} = 2.92 \times 10^{-4}$, red pentagons) has ~ 5 times fewer displacements for phononic calculations.

As pictured in Fig. 1, while the best result is achieved by the ATAT suite (olive diamonds), our best performer (green squares) gets similar results for the first five coordination zones (the latter deviate from optimal disorder).

4. Conclusions

We have proposed a modification of an established state-of-the-art tool for describing the *ab-initio* properties of alloys. By sacrificing some quantitative efficiency of describing lattice disorder, we obtain a set of Special Quasirandom Structures that perform well computationally while still modeling alloy's disorder. As in predicting new stable alloys, as well as assessing the decomposition rates [44], we need not only to calculate optimal structures for the target composition, but also its neighborhood in the composition–enthalpy-of-formation vector space. This is necessary to predict stability (as a function of external pressure p and temperature T) by studying the convex hull (CH) in the aforementioned vector space and whether the composition-of-interest lies in the convex hull (stability) or not (the distance from CH determines the decomposition rate).

The author acknowledges the continued support of Prof. Józef Spałek (Institute of Theoretical Physics, Jagiellonian University), whose insightful discussions helped to develop this research. As this work coincides with the 50-year scientific career jubilee, we wish to pay special tribute to his enduring mentorship and scientific vision.

We gratefully acknowledge Poland's high-performance infrastructure PLGrid ACK Cyfronet AGH for providing computer facilities and support within computational grant No. PLG/2025/018497. Finally, the author recognizes the help of Dominik Legut and Sergiu Arapan (IT4Innovations, VŠB — Technical University of Ostrava) in conceptualizing the problem described in this paper.

REFERENCES

[1] H. Abu-Shawareb *et al.*, «Lawson Criterion for Ignition Exceeded in an Inertial Fusion Experiment», *Phys. Rev. Lett.* **129**, 075001 (2022).

[2] A.B. Zylstra *et al.*, «Experimental achievement and signatures of ignition at the National Ignition Facility», *Phys. Rev. E* **106**, 025202 (2022).

[3] A. Saleh, R.M. Shalaby, N.A. Abdelhakim, «Comprehensive study on structure, mechanical and nuclear shielding properties of lead free Sn–Zn–Bi alloys as a powerful radiation and neutron shielding material», *Radiat. Phys. Chem.* **195**, 110065 (2022).

[4] J.S. Alzahrani *et al.*, «Nuclear shielding properties of Ni-, Fe-, Pb-, and W-based alloys», *Radiat. Phys. Chem.* **195**, 110090 (2022).

[5] A. Tasnim, M.H. Sahadath. M.N. Islam Khan, «Development of high-density radiation shielding materials containing $BaSO_4$ and investigation of the gamma-ray attenuation properties», *Radiat. Phys. Chem.* **189**, 109772 (2021).

[6] J.S. Wróbel *et al.*, «Gamma and X-ray radiation shielding of the Ta–Ti–V–W high-entropy alloy: A combined experimental and theoretical study», *Mater. Today Commun.* **51**, 114743 (2026).

[7] A.C. Souza *et al.*, «Development and Characterization of a W8Ni3Cu Alloy for Gamma Radiation Shielding», *Nucl. Technol.* **211**, 1609 (2025).

[8] P. Koželj *et al.*, «Discovery of a Superconducting High-Entropy Alloy», *Phys. Rev. Lett.* **113**, 107001 (2014).

[9] S.-G. Jung *et al.*, «High critical current density and high-tolerance superconductivity in high-entropy alloy thin films», *Nat. Commun.* **13**, 3373 (2022).

[10] C.K.W. Leung *et al.*, «Evidence for isotropic *s*-wave superconductivity in high-entropy alloys», *Sci. Rep.* **12**, 12773 (2022).

[11] R. Sereika *et al.*, «Dual-phase superconductivity in high-pressure high-temperature synthesized TaNbZrHfTi», *AIP Advances* **14**, 065216 (2024).

[12] A.P.M. Place *et al.*, «New material platform for superconducting transmon qubits with coherence times exceeding 0.3 milliseconds», *Nat. Commun.* **12**, 1779 (2021).

[13] P. Sobota *et al.*, «Superconductivity in High-Entropy Alloy System Containing Tb», *Materials* **18**, (2025).

[14] K. Jasiewicz, J. Tobola, B. Wiendlocha, «Local distortions of the crystal structure and their influence on the electronic structure and superconductivity of the high-entropy alloy $(TaNb)_{0.67}(HfZrTi)_{0.33}$», *Phys. Rev. B* **108**, 224505 (2023).

[15] K. Jasiewicz, S. Gutowska, J. Tobola, B. Wiendlocha, «Electronic Structure and Electron–Phonon Coupling Calculations for bcc HEA Superconductors Ta–Nb–Hf–Zr–Ti», in: J. Kitagawa, Y. Mizuguchi (Eds.) «High-Entropy Alloy Superconductors», Springer Series in Solid-State Sciences, Vol. 202, *Springer*, Singapore 2024, pp. 103–130.

[16] D. Smith *et al.*, «Development of vanadium-base alloys for fusion first-wall — blanket applications», *Fusion Eng. Des.* **29**, 399 (1995).

[17] R. Kurtz *et al.*, «Critical issues and current status of vanadium alloys for fusion energy applications», *J. Nucl. Mater.* **283–287**, 70 (2000).

[18] R. Neu *et al.*, «Tungsten as plasma-facing material in ASDEX Upgrade», *Fusion Eng. Des.* **65**, 367 (2003).

[19] S. Wurster, B. Gludovatz, A. Hoffmann, R. Pippan, «Fracture behaviour of tungsten–vanadium and tungsten–tantalum alloys and composites», *J. Nucl. Mater.* **413**, 166 (2011).

[20] O. El Atwani *et al.*, «A quinary WTaCrVHf nanocrystalline refractory high-entropy alloy withholding extreme irradiation environments», *Nat. Commun.* **14**, 2516 (2023).

[21] M. Mo *et al.*, «Direct observation of strong momentum-dependent electron–phonon coupling in a metal», *Sci. Adv.* **10**, eadk9051 (2024).

[22] C. Acemi *et al.*, «Multi-objective, multi-constraint high-throughput design, synthesis, and characterization of tungsten-containing refractory multi-principal element alloys», *Acta Mater.* **281**, 120379 (2024).

[23] G. Wei *et al.*, «Revealing the critical role of vanadium in radiation damage of tungsten-based alloys», *Acta Mater.* **274**, 119991 (2024).

[24] C. Hatler *et al.*, «The path towards plasma facing components: A review of state-of-the-art in W-based refractory high-entropy alloys», *Curr. Opin. Solid State Mater. Sci.* **34**, 101201 (2025).

[25] M. Wurmshuber *et al.*, «Small-scale fracture mechanical investigations on grain boundary doped ultrafine-grained tungsten», *Acta Mater.* **250**, 118878 (2023).

[26] A. Mackova *et al.*, «Radiation damage evolution in High Entropy Alloys (HEAs) caused by 3–5 MeV Au and 5 MeV Cu ions in a broad range of dpa in connection to mechanical properties and internal morphology», *Nucl. Mater. Energy* **37**, 101510 (2023).

[27] P. Hohenberg, W. Kohn, «Inhomogeneous Electron Gas», *Phys. Rev.* **136**, B864 (1964).

[28] W. Kohn, L.J. Sham, «Self-Consistent Equations Including Exchange and Correlation Effects», *Phys. Rev.* **140**, A1133 (1965).

[29] W. Kohn, «Electronic Structure of Matter-Wave Functions and Density Functionals», 1998, Nobel Prize lecture, `https://www.nobelprize.org/prizes/chemistry/1998/kohn/lecture/`

[30] A.I. Liechtenstein, V.I. Anisimov, J. Zaanen, «Density-functional theory and strong interactions: Orbital ordering in Mott–Hubbard insulators», *Phys. Rev. B* **52**, R5467 (1995).

[31] S.L. Dudarev *et al.*, «Electron-energy-loss spectra and the structural stability of nickel oxide: An LSDA+U study», *Phys. Rev. B* **57**, 1505 (1998).

[32] G. Kotliar *et al.*, «Electronic structure calculations with dynamical mean-field theory», *Rev. Mod. Phys.* **78**, 865 (2006).

[33] D. Vollhardt, «Dynamical mean-field theory for correlated electrons», *Ann. Phys.* **524**, 1 (2012).

[34] A. Zunger, S.H. Wei, L.G. Ferreira, J.E. Bernard, «Special quasirandom structures», *Phys. Rev. Lett.* **65**, 353 (1990).

[35] S.H. Wei, L.G. Ferreira, J.E. Bernard, A. Zunger, «Electronic properties of random alloys: Special quasirandom structures», *Phys. Rev. B* **42**, 9622 (1990).

[36] C. Jiang, «First-principles study of ternary bcc alloys using special quasi-random structures», *Acta Mater.* **57**, 4716 (2009).

[37] M. Lebeda *et al.*, «SimplySQS: An Automated and Reproducible Workflow for Special Quasirandom Structure Generation with ATAT», https://atat-sqs.streamlit.app/

[38] C. Niu, L. Liu, «Short-range order based ultra fast large-scale modeling of high-entropy alloys», *Comput. Mater. Sci.* **253**, 113792 (2025).

[39] A. van de Walle, «Multicomponent multisublattice alloys, nonconfigurational entropy and other additions to the Alloy Theoretic Automated Toolkit», *Calphad* **33**, 266 (2009).

[40] D. Gehringer, M. Friák, D. Holec, «Models of configurationally-complex alloys made simple», *Comput. Phys. Commun.* **286**, 108664 (2023).

[41] Y. Hao *et al.*, «Inverse Materials Design by Large Language Model-Assisted Generative Framework», arXiv:2502.18127 [cond-mat.mtrl-sci].

[42] S. Zhang *et al.*, «Constructing material network representations for intelligent amorphous alloy design», *Natl. Sci. Rev.* **12**, nwaf398 (2025).

[43] A.P. Kądzielawa, D. Legut, «On the miscibility gap in tungsten-based alloys», *Int. J. Refract. Met. Hard Mater.* **115**, 106272 (2023).

[44] J. Veverka *et al.*, «Decreasing the W–Cr solid solution decomposition rate: Theory, modelling and experimental verification», *J. Nucl. Mater.* **576**, 154288 (2023).

[45] H.C. Andersen, «Cluster Methods in Equilibrium Statistical Mechanics of Fluids», in: B.J. Berne (Ed.) «Statistical Mechanics. Part A: Equilibrium Techniques», Modern Theoretical Chemistry, Vol. 5, *Springer*, Boston, MA 1977, pp. 1–45.

[46] A. Togo, L. Chaput, I. Tanaka, G. Hug, «First-principles phonon calculations of thermal expansion in Ti_3SiC_2, Ti_3AlC_2, and Ti_3GeC_2», *Phys. Rev. B* **81**, 174301 (2010).

[47] A. Togo, I. Tanaka, «First principles phonon calculations in materials science», *Scr. Mater.* **108**, 1 (2015).

[48] N. Metropolis *et al.*, «Equation of State Calculations by Fast Computing Machines», *J. Chem. Phys.* **21**, 1087 (1953).